Vietnam Journal of Catalysis and Adsorption
Tạp chí xúc tác và hấp phụ Việt Nam

http://chemeng.hust.edu.vn/jca/

Enhanced photocatalytic degradation performance of bisphenol A over TiO_2-SiO_2 photocatalyst by improving specific surface area under simulation natural light

Minh-Vien Le[1,2*]Huynh Huu Tai[1,2], Nguyen Thi Kieu Oanh[1,2], Ngo Manh Thang[1,2], Ho Thi Ngoc Suong[1,2]

[1] *Faculty of Chemical Engineering, Ho Chi Minh city University of Technology, Ho Chi Minh City, 700000, Vietnam*
[2] *Vietnam National University Ho Chi Minh City, Ho Chi Minh City,700000, Vietnam*
**Email: lmvien@hcmut.edu.vn*

ARTICLE INFO

Received: 16/7/2020
Accepted: 30/8/2020

Keywords:
TiO_2-SiO_2 photocatalyst, Bisphenol A, Simulated Natural Light.

ABSTRACT

The application of natural light in photocatalytic process is a potential energy source. In this study, TiO_2-SiO_2 nanoparticles with outstandingly enhanced photocatalytic activity have been fabricated by sol-gel method. The prepared photocatalysts with different molar ratio of TiO_2:SiO_2 as 100:0; 95:5; 85:15 and 75:25 were denoted as TiO_2, TS5, TS15 and TS25, respectively. Characterization of these photocatalysts was evaluated using transmission electron microscopy (TEM), X-ray diffraction (XRD), N_2 Adsorption and Desorption isotherms method (Brunauer–Emmet–Teller, BET). The specific surface area was improved in TiO_2-SiO_2 photocatalyst namely 193.9 $m^2.g^{-1}$ (at molar ratio of TiO_2:SiO_2 of 95:5) compared to 33.6 $m^2.g^{-1}$ of TiO_2. The crystallite size was calculated around 5 nm from XRD data and uniform particle size distribution was observed in TEM image. The photocatalytic experiments were performed with bisphenol A (BPA) as model compound of organic pollutant. The effect of various operation parameters such as initial concentration, initial solution pH and photocatalyst dosage has been investigated. The kinetic studies of the photocatalytic degradation BPA over TS5 followed the pseudo-first order ($k=1.09\times10^{-2}$ min^{-1}) and degradation yield to be 82.4% BPA, at pH6.23, initial concentration to be 10 ppm and photocatalyst dosage to be 1.0 $g.L^{-1}$. The photocatalyst TS5 maintained activity after four cycles and remained 78%. The TiO_2-SiO_2 composite photocatalyst has shown to be a promising heterogeneous photocatalyst for organic degradation.

Introduction

In recent decades, environmental pollution has been receiving a great deal of public attention. Especially, the toxic organic compound in wastewater can affect directly to human health through water environment, thus some feasible solutions were developed to solve these problems such as photocatalysis [1-4], adsorption [5], adsorption – photocatalysis [6], photoelectrical oxidation [7], etc. Along with the development of hybrid semiconductor photocatalyst, titanium dioxide (TiO_2) as semiconductor has been studied as a base material to combine with other materials to improve its defects like small surface area, low adsorption of toxic organic compound and phase stability at high calcined temperature [8]. Therefore, the development for a

http://doi.org/10.51316/jca.2020.069

material that can improve the TiO_2 surface area and phase stabilization needs to be studied.

The combination of SiO_2 also contributes significantly to increasing the specific surface area of the material, so that the ability to adsorb pollutants to the catalytic surface is enhanced. Many researchers have been reported their studies about TiO_2-SiO_2 hybrid material and achieved remarkable results. Vaithiyanathan Ramamoorthy and colleagues synthesized successfully TiO_2-SiO_2 composite photocatalyst, the composite photocatalyst 30% w/w TiO_2-SiO_2 have outstandingly enhanced specific surface area, namely 279 $m^2.g^{-1}$ as compare to 92 $m^2.g^{-1}$ of pure TiO_2. Accordingly, the percentage decolorizations of acid orange (AO20) were 67% and 89% for pure TiO_2 and 30% w/w TiO_2-SiO_2, respectively. This result may be due to higher surface area [9]. In another research, Vinayak G. Parale and coworkers was synthesized hydrophobic TiO_2-SiO_2 composite aerogels via in-situ polymerization and sol-gel process, according that the molar ratio of TiO_2:SiO_2 to be 0.7:1.0. Furthermore, the specific surface areas were 62 $m^2.g^{-1}$ and 252 $m^2.g^{-1}$ for TiO_2 and TiO_2-SiO_2 composite, respectively. The degradation efficiency of methylene blue (MB) was obtained 57% and 87% after 90 min under UV irradiation for TiO_2 and TiO_2:SiO_2 composite [10], respectively. Moreover, the enhancing surface areas when combine SiO_2 and TiO_2 was also observed in many research [11-14]. It has been proved that the important role of SiO_2 in improvement specific surface of photocatalyst.

Bisphenol A ($(CH_3)_2C(C_6H_4OH)_2$, BPA), which is raw material for plastic manufacture, especially polycarbonate plastic and epoxy resins [15-17]. It can be discharged into the water and/or air environment during manufacturing. Besides, amount of residual BPA can release from plastic products to environment directly effecting to human health [15]. In recent decade, the application photocatalysis process in BPA degradation have been developed in many reports [18-21]. The photocatalytic material has many advantages, its structure can be doped with metal or nonmetal to enhance light adsorption intensity, BPA can be partially or completely degraded. Also, after BPA degradation, the photocatalyst can reuse after many uses. In the recent year, many researchers have reported their efforts to improve BPA removal efficiency. Particularly, Chao-Yin Kuo and colleagues synthesized C-doped TiO_2 (C-TiO_2) photocatalyst for degradation BPA under sunlight irradiation, as follow this research, the band gap energy of C-TiO_2 (molar ratio of C:Ti of 0.05:1) reduced significantly to 2.92 eV and the reaction rate constant was estimated to be 2.08 h^{-1}. However, the specific surface of C-TiO_2 is quite low, just be 46.4 $m^2.g^{-1}$ event at low calcination temperature of 450 ^oC [22]. In another research, Shepherd Sambaza and coworkers studied BPA photocatalytic degradation on polyaniline (PANI) supported Ag@TiO_2 (Ag@TiO_2-PANI) nanocomposite. The Ag@TiO_2-PANI composite was achieved band gap energy of 3.0 eV and the yield of BPA degradation up to 99.7% under visible light irradiation. This outstandingly achievement may be due to the presence of Ag nanoparticles on TiO_2 surface made recombination of electron and hole reduce. However, the specific surface of Ag@TiO_2-PANI was pretty low 52.5 $m^2.g^{-1}$ [20]. Finally, BPA degradation have been investigated in many researches, but the improvement in surface area, which is an important factor in photocatalytic process has not yet been focused.

In this research, we focus on enhancing the BET surface area of the photocatalytic process. The combination of SiO_2 with TiO_2 in TiO_2-SiO_2 photocatalyst make the photocatalyst achieved large specific surface area a factor effect directly to adsorption, which is the first step of photocatalytic process. Furthermore, the presence of SiO_2 also improves phase stability. The photocatalytic activity experiments were tested in slurry reactor. Additionally, different operation parameters were investigated as initial BPA solution pH, photocatalyst dosage, initial BPA concentration. Besides, to increase practical applicability, the photocatalyst was undergone reuse experiment.

Experimental

Material

Reactants such as Tetraethyl orthosilicate (TEOS, ≥ 99%, Merck, Germany), tetra-n-butyl orthotitanate (TNB, ≥ 99%, Acros Organics), polyethylene glycol 20000 (PEG 20000, Sigma-Aldrich, Germany), acid nitric (HNO_3, 65%, Merck, Germany), absolute ethanol (C_2H_5OH, ≥ 99.5%, Vietnam), acetyl acetone (AcAc, ≥ 99%, Merck), Bis-phenol A (BPA, ≥ 99%, Sigma-Aldrich) were used as received without any purified step.

Photocatalyst preparation

Photocatalyst materials TiO_2-SiO_2 were synthesized by sol-gel method. Firstly, solution included 4.00 g of TNB, 1.2 mL of AcAc, 5.0 mL of Ethanol and 0.5 mL of HNO_3 65 wt.% was kept at 80 ^oC under magnetic stirring for 1h to form homogeneous solution A. At the same time, solution B including TEOS, 0.20 g of PEG, 5.0 mL of

Ethanol, 0.5 mL of HNO_3 65 wt.% and 2.4 mL of deionized water was prepared under magnetic stirring. Amount of TEOS was designed so that the molar ratio of TiO_2:SiO_2 of 95:5; 85:5, 75:25 and denoted as TS5, TS15, TS25, respectively. Subsequently, solution A was added dropwise into solution B and kept stirring for 2h. Finally, TiO_2-SiO_2 solution was dried at 120 ^oC for 3h and then calcined at 500 ^oC for 2h. For comparison, TiO_2 powder was also synthesized without using TEOS.

Characterization

The phase compositions and crystal structures of the samples were determined by X-ray diffraction (XRD) using a D2 Phaser (Bruker, USA) with Cu-Kα radiation (λ = 0.154 nm). The equipment operates at the step size of 0.02 ° at the rate of 0.2 °/s. The calculated crystallite size was determined by the Scherrer equation (Eq. 1) at (101) peak. In which β is the full width at half-maximum of the diffraction peak (FWHM), k=0.9 is a shape constant, D is the crystallite size and θ is the Bragg angle.

$$D = \frac{k\lambda}{\beta \cos\theta} \quad (1)$$

The N_2 adsorption-desorption isotherms were carried out at 77K by Quantachrome NOVA 1000E. The BET specific surface was determined from data over the relative pressure (P/P_o) ranging from 0.046 to 0.986. The TEM image was obtained by using FE-SEM JEOL 7401.

The zero-point charge (pH_{ZPC}) was determined as a previous study [23]. Firstly, 25 mL KCl 0.1N and diluted with distilled water to obtain 100 mL of solution with designed pH values (pH_i): 3, 4, 6, 7, 8, 9 by HCl 0.1N or NaOH 0.1N respectively. Secondly, the prepared solutions were added into the separated beaker, which contained 0.10 g of photocatalyst per each. The mixtures were stirred for 48h at speed of 180 rpm, then filtered with filter paper to remove the photocatalyst and recorded pH value (pH_f). The pH variation (ΔpH) was calculated as the following equation (Eq.2):

$$\Delta pH = pH_f - pH_i \quad (2)$$

Photocatalytic activity

The photocatalytic activities of photocatalysts were evaluated through the degradation of 200 mL BPA solution with initial concentration to be 10 $mg.L^{-1}$ under simulated natural light using a 25 W lamp (Natural light PT 2191-ExoTerra). The reactions were carried out in a slurry reactor, the suspension containing BPA solution and photocatalysts was continuously stirred for 1h to achieve adsorption-desorption equilibrium. Following, the suspension has been irradiated to performing photocatalytic reactions. During this process, the suspension was stirred continuously and the temperature was maintained around 30 ^oC using a cooling water jacket. An aliquot suspension was extracted from the reactor at the designed time and separated using 0.45 μm springe filter for determining residual BPA concentration. For testing reusability, after each cycle, the photocatalyst was separated from the suspension by centrifugation, then dried at 120 ^oC and following calcined at 350 ^oC to evaporate residual BPA and other organic compounds before using for the next cycle. The residual BPA concentration was determined using Hitachi UV-Vis spectrometer equipment. The absorbance of BPA has been measured at a characteristic absorption wavelength of 225 nm. The BPA photocatalytic degradation efficiency was calculated as the following equation (Eq. 3):

$$H(\%) = \left(1 - \frac{A}{A_o}\right).100\% \quad (3)$$

where A_0 and A are the absorbance at 225 nm of characteristic wavelength of the BPA solution before and after irradiation, respectively.

To estimate the mass of photocatalyst needs for the photocatalytic experiment, the experiments were performed with different TS5 photocatalyst dosage which were 0.25 to 2.00 $g.L^{-1}$ of BPA solution with initial concentration of 10$mg.L^{-1}$ and natural pH to be 6.23. The effect of the initial concentration of BPA was investigated in the range from 10 to 40 $mg.L^{-1}$ and the photocatalyst dosage of 0.50 $g.L^{-1}$. To account for the effect of initial pH on the photocatalytic degradation of BPA on TS5 photocatalyst, the 10 $mg.L^{-1}$ of BPA solution was prepared and adjusted pH in the range from 4 to 8 and the photocatalyst dosage of 0.50 $g.L^{-1}$.

To investigate BPA photocatalytic degradation reaction kinetic, the BPA solution was determined concentration after every 30 min.

The Langmuir–Hinshelwood (L – H) kinetic model is expressed as Eq. (4) and is used to examine the kinetics of photocatalytic reactions [24]:

$$r = -\frac{dC}{dt} = \frac{k_r K_a C}{1 + K_a C} \quad (4)$$

where k_r (min^{-1}), K_a and C (mg/L) are the rate constant, Langmuir absorption constant and concentration of contaminant, respectively. At a very low concentration

of BPA (lower than 40 mg.L^{-1}), the solution can be seen as a diluted aqueous solution so KC<<1. The L-H equation can be simplified to pseudo-first order equation (Eq. 5) as follow:

$$\ln\left(\frac{C}{C_o}\right) = kt \quad (5)$$

where k is the reaction rate constant, C is the residual BPA concentration and the concentration, C_o is the concentration of BPA solution when the light was turned on.

Results and discussion

Figure 1 shows the XRD pattern of TiO_2-SiO_2 samples and pure TiO_2 were calcined at 500 °C for 2h. As shown, all identical peaks at 2θ diffraction angles of 25.2° (101), 36.9° (004), 48.2° (200), 54.8° (211) and 63.0° (204) can be attributed to the anatase TiO_2 (Anatase – JCPDS-21-1272) and no characteristic peak of rutile was observed. Besides, no typical peak of SiO_2 was detected, this indicates that SiO_2 is present in an amorphous phase.

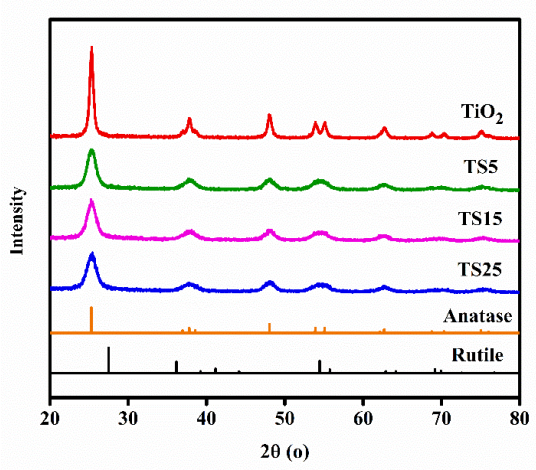

Figure 1: XRD pattern of pure TiO_2 and TiO_2-SiO_2 samples

The average crystallite size of the prepared particles is given in Table 1. Crystallite sizes of TiO_2-SiO_2 photocatalysts are smaller than that of pure TiO_2 and decrease with increasing SiO_2 concentration. This phenomenon is attributed to the formation of Si-O networks by excessive SiO_2, which prevents the production of anatase crystallites because the TiO_2 in the anatase phase cannot contact with isomorphous octahedral site substitution to forming rutile phase [25].

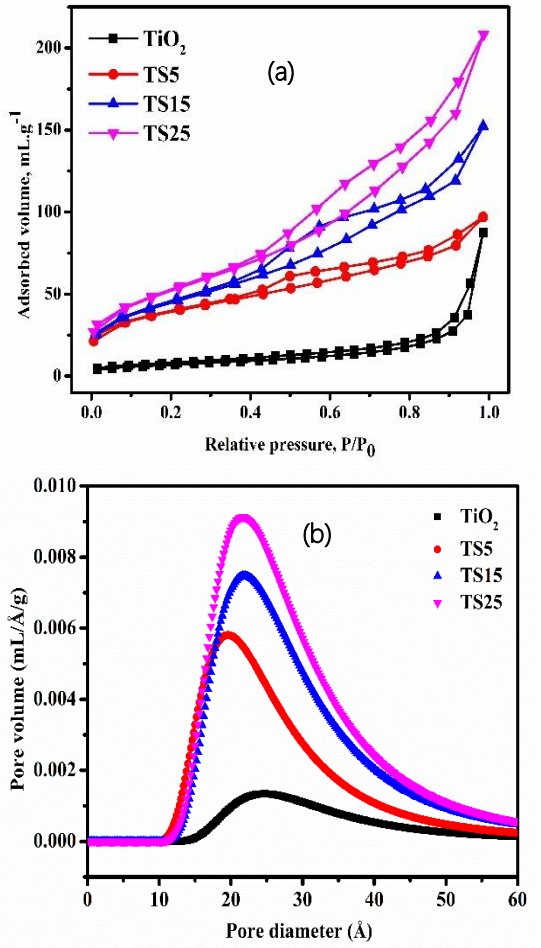

Figure 2: (a) N_2 adsorption-desorption isotherms and (b) DA analysis of TiO_2, TS5, TS15 and TS25 photocatalysts

Table 1: Crystallite size, BET surface and porous parameter of TiO_2 and TiO_2-SiO_2 samples

Photocatalyst	Average crystallite size (nm)	SSA ($m^2.g^{-1}$)	Pore volume ($mL.g^{-1}$)	Pore diameter (nm)
TiO_2	16	33.6	0.138	1.5
TS5	6	193.9	0.158	1.2
TS15	6	209.2	0.245	2.7
TS25	5	247.8	0.336	2.0

The microstructural properties of TiO_2-SiO_2 the photocatalyst with different molar ratios were investigated using N_2 adsorption-desorption isotherms at 77K and Dubinin-Astakhov (DA) method micropore analysis from the desorption profiles of TiO_2 and TiO_2-SiO_2 photocatalysts. These samples indicated a type IV isotherm with a H3 hysteresis loop, characteristic of the combination of the microporous material. The BET surface areas were determined to be 33.6, 193.9, 209.2 and 247.8 $m^2.g^{-1}$ for TiO_2, TS5, TS15 and TS25, respectively. The significant increase in specific surface area was observed in the presence of SiO_2. The higher specific surface contributed multiple active sites and improved adsorption capacity, which are important in the photocatalytic process.

To clearly observe the crystal structure, the TEM images of TS5 and TS25 photocatalyst were taken and showed in Figure 3. The TEM images indicate that the TS5 and TS25 nanoparticles considered of spherical shape, and the average particle diameter was estimated about 10 – 15 nm and the uniform distribution of nanoparticles was observed. Although there may have been agglutination between the crystals, the TEM image still showed a smaller particle size than TiO_2 (16 nm), this can be attributed by the role of SiO_2 in photocatalyst. During the calcination process, the SiO_2 can be incorporated with TiO_2 and was forming gradually a layer coating on the TiO_2 surface, therefore, the crystallite size was reduced [8]. This phenomenon was consistent with the results obtained from XRD pattern.

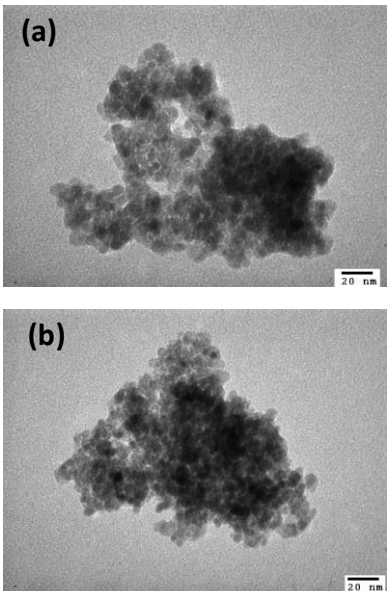

Figure 3: TEM images of the prepared TiO_2-SiO_2 particles: (a) TS5 and (b) TS25

Effect of TiO_2:SiO_2 molar ratio

Figure 4 shows the comparison of photocatalytic activities of various TiO_2-SiO_2 photocatalysts. It can be seen from Figure 4, in the absence of the photocatalyst, BPA is stable under photolysis irradiation. During the photocatalytic process, almost photocatalyst can degrade BPA at any molar ratio, the TiO_2-SiO_2 catalyst indicated enhancing adsorption capacity rather than pure TiO_2 photocatalyst as a result of SiO_2 combination. After 240 min reaction, the experimental results show that the TS5 photocatalyst achieved the greatest photocatalytic activity, this result corresponding to previous research [26-29]. The decreased activity in TS25 photocatalyst may be due to the excess SiO_2 leaches out the photocatalyst, another reason can be attributed by SiO_2 overlay the activity site of TiO_2 at high content. This result shows an improvement in photocatalytic activity when combining a small amount of SiO_2.

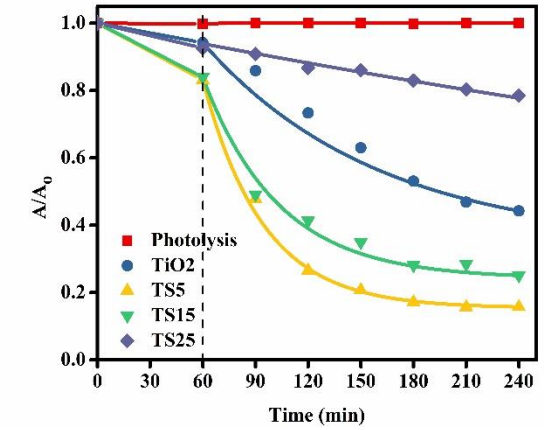

Figure 4: Effect of various ratios of TiO_2:SiO_2 on photocatalytic degradation efficiency at C_{BPA}=10 $mg.L^{-1}$, photocatalyst dosage=1.0 $g.L^{-1}$, V_{BPA}=200 mL

Effect of photocatalyst dosage

The effect of photocatalyst dosage was carried out with TS5 photocatalyst in the range from 0.25 to 2.0 $g.L^{-1}$ at a BPA initial concentration of 10 $mg.L^{-1}$. The results were shown in Figure 5, according to that the photocatalyst dosage of 1.00 $g.L^{-1}$ shows the highest reaction rate constant and degradation efficiency. The phenomena can be explained when the photocatalyst dosage increase from 0.25 to 1.00 $g.L^{-1}$, increasing the amount of TS5 leads to a larger number of active sites that mean more than radicals were formed. Otherwise, increasing the photocatalyst dosage from 1.00 to 2.00 $g.L^{-1}$ reduces the degradation efficiency of BPA, this may be due to the increasing turbidity of the solution along with excess photocatalyst [30]. The increasing

http://doi.org/10.51316/jca.2020.069

turbidity makes photon flux cannot active the photocatalyst resulting in less than radicals.

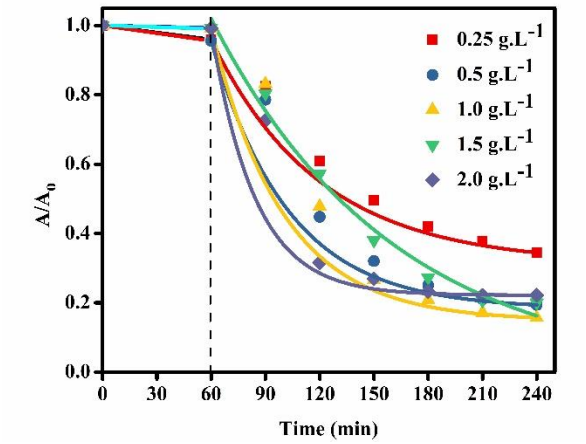

Figure 5: Effect of TS5 dosage on BPA degradation under simulated natural light at C_{BPA}=10 mg.L^{-1}, V_{BPA}=200 mL, pH6.23

Effect of initial pH of BPA solution

The pH of the solution is an important parameter influence the adsorption behavior in the photocatalytic process. The pH value will determine the concentration of OH^- species, which is the precursor to the formation of hydroxyl radicals oxidizing agents in the photocatalyst process. The pH value also affects to the BPA form, when the pH lower than pKa (9.58) the BPA exists in its neutral form ($(CH_3)_2C(C_6H_4OH)_2$), on the contrary, the ionic BPA is formed ($(CH_3)_2C(C_6H_4O^-)_2$) [31]. Besides, the surface charge properties determined by the zero-point charge enhances the interaction between photocatalyst and organic pollutant [32]. The experimental results determine the zero-point charge was shown in Figure 6, according to that the pH_{ZPC} was estimated to be 5.89.

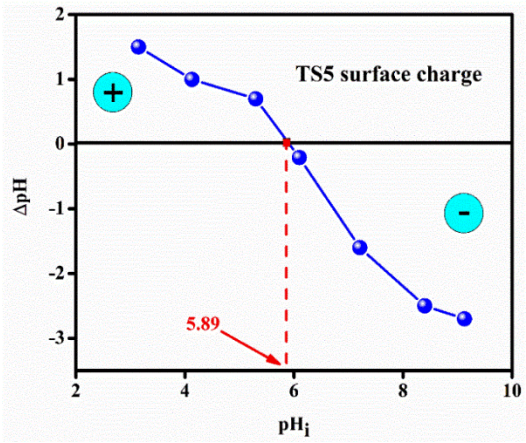

Figure 6: TS5 zero-point charge estimation diagram

The experiment evaluated the effect of pH was carried out in the range from 4 to 8. The results were presented in Figure 7, the highest BPA degradation was documented at the original pH value of 6.23 as the comparison with the others pH values. This result can be explained by the acidic environment pH lower 5.89 make the TS5 surface charge is positive, while BPA exists in neutral form. The positively charged surface formation of TS5 is occupied with H^+ ions, accordingly increasing the formation of hydroxyl radicals and increase BPA adsorption onto the photocatalyst surface may be due to electrostatic interaction between positive surface and phenolic ring in BPA structure [33]. As increasing pH values, when pH values higher than pH_{ZPC} the surface charge was inverted to negative, the adsorption BPA will be reduced cause both the photocatalyst surface and phenolic ring of BPA were negatively charged, and naturally, reduce BPA degradation efficiency. The reducing BPA degradation efficiency at a weak basic environment was similarly demonstrated in research of Blanco-Vega and co-workers when study Ni-doped TiO_2 photocatalyst [34].

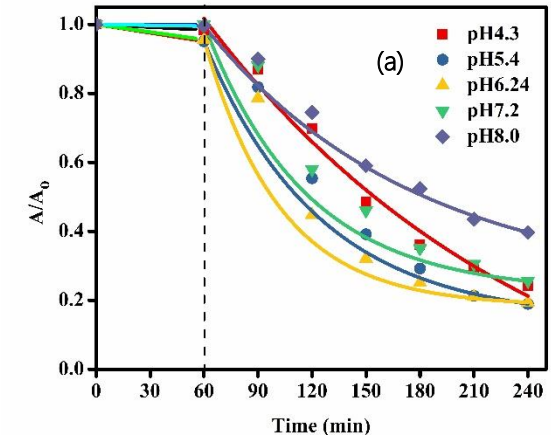

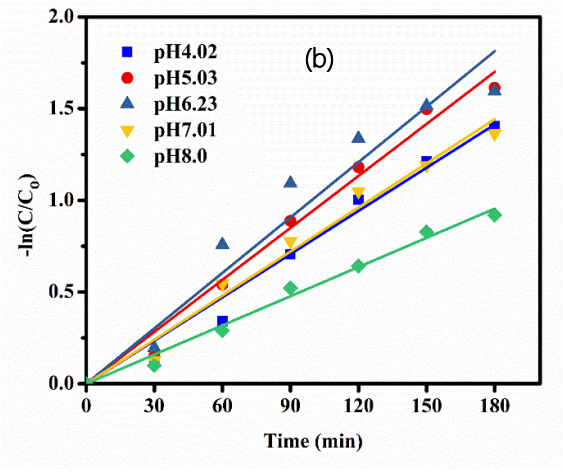

Figure 7: (a) Effect of initial pH on BPA degradation under simulated natural light; (b) Plot of -ln(C/C_o) versus time for estimate reaction rate constant

Effect of initial concentration of BPA solution

The effect of the initial concentration of BPA on the degradation of BPA under the simulated solar light was later determined. Because BPA is a weak acid with two hydroxyl groups in structure, so the pH value was not changed significantly along increasing BPA concentration. The obtained results have been presented in Figure 8. The results indicated that the degradation efficiency and reaction rate constant reduce along with increasing BPA concentration. According to shown in Table 2, a significant change in the reaction was observed between two concentrations 20 and 30 mg.L^{-1}. The reason can be explained as two factors having a dependent effect on the photocatalytic process, the density of BPA was adsorption and the intensity of light absorbed on the TS5 surface. When the BPA concentration below 20 mg.L^{-1}, BPA molecules in solution will have good contact with photocatalyst and the photons can be easily absorbed by photocatalyst. However, when the BPA concentration above 30 mg.L^{-1}, the BPA molecules become excess lead to the photons were interrupted before reach with photocatalyst as consequently reduce the BPA degradation efficiency [35]. Similar results were demonstrated by Lin Yanyan and colleagues when investigating the effect of acetaminophen initial concentration to degradation performance on $WO_3/TiO_2/SiO_2$ composite under UV-Vis irradiation [29]. According to this research, the related development was recognized in a concentration range from 10 to 15 mg.L^{-1}. Hence the maximum suitable concentration for which the catalyst can well maintain the photocatalytic capacity is 20 mg.L^{-1}.

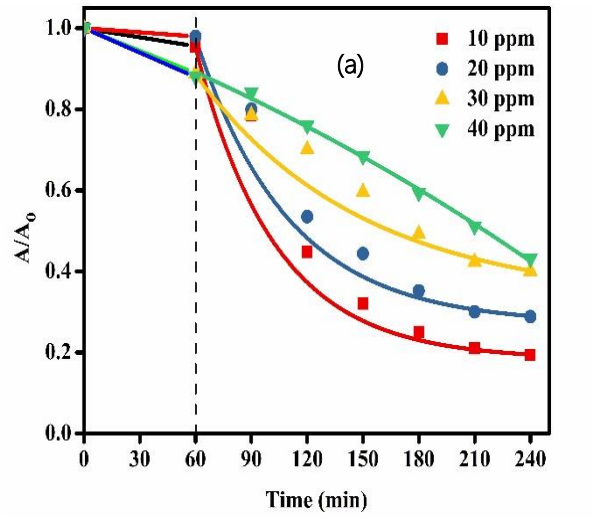

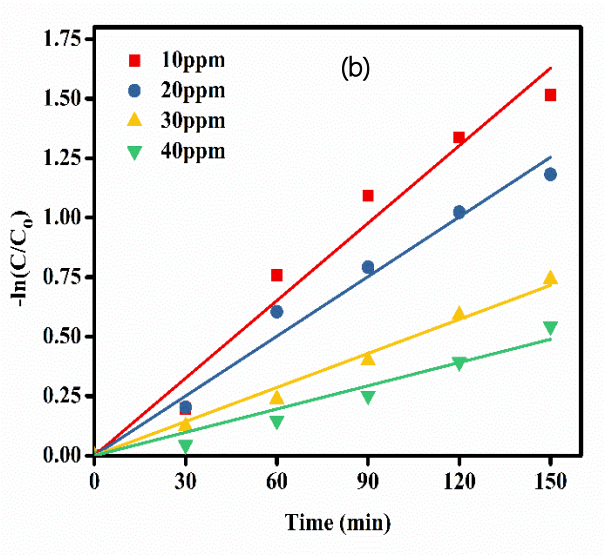

Figure 8: (a) Effect of BPA concentration on BPA degradation at pH6.23, photocatalyst dosage = 1.0 g.L^{-1}, V_{BPA} = 200 mL (b) Plot of -ln(C/C_o) versus time for estimate reaction rate constant

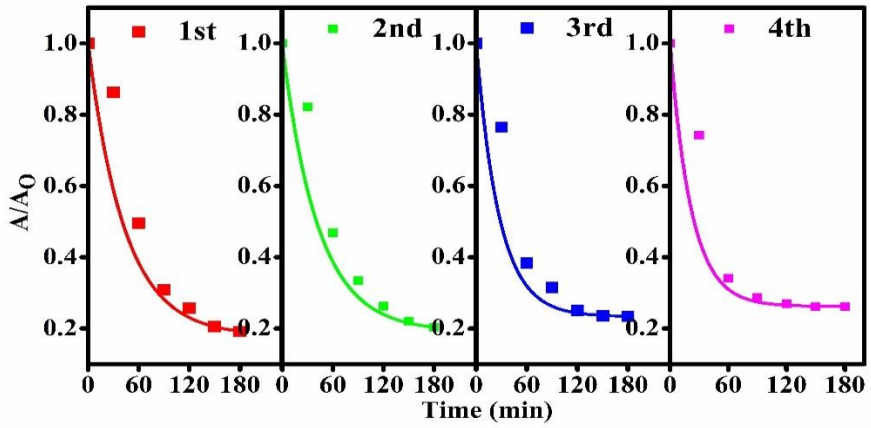

Figure 9: Recycling test of TS5 for photocatalytic degradation BPA at C_{BPA}=10 mg.L^{-1}, photocatalyst dosage=1.0 g.L^{-1}, pH6.23, V_{BPA}=200 mL

Table 2: Reaction rate constant for BPA degradation at different initial concentrations

Initial BPA concentration ($mg.L^{-1}$)	Reaction rate constant (min^{-1})	R^2
10	0.0109	0.990
20	0.0084	0.994
30	0.0048	0.996
40	0.0034	0.981

Reusability test

To evaluate the reusability of TS5 photocatalyst, the experiments were performed on TS5 photocatalyst and the results of four times test were displayed in Figure 9. To prepare for next run, the weight loss would be compensated from an experiment that was run in parallel under the same conditions. Especially, after four times reuse, the degradation efficiency was remained 78%.

Conclusion

Through this research, TiO_2-SiO_2 photocatalyst was prepared, characterized and tested photocatalytic activity on degradation BPA under simulated natural light. The important roles of SiO_2 in phase stability were observed in the XRD pattern. As above synthesizing procedure, the TiO_2:SiO_2 photocatalyst with molar ratio of 95:5 achieved a large surface to be 193.9 and a small crystalline size of 6 nm. BPA was degraded 82.4% after 4h irradiation, and maintained 78% after four times reuse under initial concentration up to 20 $mg.L^{-1}$, natural pH of 6.23

Acknowledgments

This research is funded by Vietnam National University HoChiMinh City (VNU-HCM), under grant number 562-2018-20-02.

References

1. M. C. Ortega-Liebana et al., Extraordinary sensitizing effect of co-doped carbon nanodots derived from mate herb: Application to enhanced photocatalytic degradation of chlorinated wastewater compounds under visible light, 218, (2017) 68-79. https://doi.org/10.1016/j.apcatb.2017.06.021
2. Y. He, N. B. Sutton, H. H. Rijnaarts, and A. A. J. A. C. B. E. Langenhoff, Degradation of pharmaceuticals in wastewater using immobilized TiO_2 photocatalysis under simulated solar irradiation, 182, (2016) 132-141,. https://doi.org/10.1016/j.apcatb.2015.09.015
3. S. Chakraborty et al., Photocatalytic hollow fiber membranes for the degradation of pharmaceutical compounds in wastewater, 5, 5, (2017) 5014-5024,. https://doi.org/10.1016/j.jece.2017.09.038
4. Z. Wu, X. Yuan, J. Zhang, H. Wang, L. Jiang, and G. J. C. Zeng, Photocatalytic decontamination of wastewater containing organic dyes by metal–organic frameworks and their derivatives, 9, 1, (2017) 41-64,. https://doi.org/10.1002/cctc.201600808
5. S. Xu, Y. Lv, X. Zeng, and D. J. C. E. J. Cao, ZIF-derived nitrogen-doped porous carbons as highly efficient adsorbents for removal of organic compounds from wastewater, 323, (2017) 502-511. https://doi.org/10.1016/j.cej.2017.04.093
6. N. Mukwevho et al., Removal of naphthalene from simulated wastewater through adsorption-photodegradation by ZnO/Ag/GO nanocomposite, 81, (2020) 393-404. https://doi.org/10.1016/j.jiec.2019.09.030
7. P. Li et al., Ternary semiconductor metal oxide blends grafted Ag@ AgCl hybrid as dimensionally stable anode active layer for photoelectrochemical oxidation of organic compounds: Design strategies and photoelectric synergistic mechanism, 362, (2019) 336-347. https://doi.org/10.1016/j.jhazmat.2018.09.041
8. K. Okada, N. Yamamoto, Y. Kameshima, A. Yasumori, and K. J. J. J. o. t. A. C. S. MacKenzie, Effect of silica additive on the anatase-to-rutile phase transition, 84, 7, (2001) 1591-1596,. https://doi.org/10.1111/j.1151-2916.2001.tb00882.x
9. V. Ramamoorthy, K. Kannan, A. I. Joice Joseph, T. Kanagaraj, S. J. J. o. N. Thiripuranthagan, and Nanotechnology, Photocatalytic degradation of acid orange dye using silver impregnated TiO_2/SiO_2 composite catalysts, 16, 9, (2016) 9980-9986. https://doi.org/10.1166/jnn.2016.12071
10. V. G. Parale, T. Kim, K.-Y. Lee, V. D. Phadtare, R. P. Dhavale, and H.-H. J. C. I. Park, Hydrophobic TiO_2–SiO_2 composite aerogels synthesized via in situ epoxy-ring opening polymerization and sol-gel process for enhanced degradation activity, 46, 4, (2020) 4939-4946. https://doi.org/10.1016/j.ceramint.2019.10.231
11. F. Li, B. Cao, R. Ma, J. Liang, H. Song, and H. J. T. C. J. o. C. E. Song, Performance of Cu/TiO_2-SiO_2 catalysts in hydrogenation of furfural to furfuryl alcohol, 94, 7, (2016) 1368-1374. https://doi.org/10.1002/cjce.22503
12. X. Chen, H. Sun, J. Zhang, Y. Guo, and D.-H. J. J. o. M. L. Kuo, Cationic S-doped TiO_2/SiO_2 visible-light photocatalyst synthesized by co-hydrolysis method and its application for organic degradation, 273, (2019) 50-57. https://doi.org/10.1016/j.molliq.2018.10.021
13. A. Pourzad, H. R. Sobhi, M. Behbahani, A. Esrafili, R. R. Kalantary, and M. J. J. o. M. L. Kermani, Efficient visible light-induced photocatalytic removal of paraquat using N-doped TiO_2@ SiO_2@ Fe_3O_4 nanocomposite,

299, (2020) 112167. https://doi.org/10.1016/j.molliq.2019.112167
14. E. Mrotek, S. Dudziak, I. Malinowska, D. Pelczarski, Z. Ryżyńska, and A. J. S. o. T. T. E. Zielińska-Jurek, Improved degradation of etodolac in the presence of core-shell $ZnFe_2O_4/SiO_2/TiO_2$ magnetic photocatalyst, (2020) 138167. https://doi.org/10.1016/j.scitotenv.2020.138167
15. C. A. Staples, P. B. Dome, G. M. Klecka, S. T. Oblock, and L. R. J. C. Harris, A review of the environmental fate, effects, and exposures of bisphenol A, 36, 10, (1998) 2149-2173. https://doi.org/10.1016/S0045-6535(97)10133-3
16. A. V. Krishnan, P. Stathis, S. F. Permuth, L. Tokes, and D. J. E. Feldman, Bisphenol-A: an estrogenic substance is released from polycarbonate flasks during autoclaving, 132, 6, (1993) 2279-2286. https://doi.org/10.1210/endo.132.6.8504731
17. L.-C. Wang, X.-j. Ni, Y.-H. Cao, and G.-q. J. A. S. S. Cao, Adsorption behavior of bisphenol A on CTAB-modified graphite, 428, 165-170, 2018. https://doi.org/10.1016/j.apsusc.2017.07.093
18. H. Wang et al., Preparing a photocatalytic Fe doped TiO_2/rGO for enhanced bisphenol A and its analogues degradation in water sample, 505, p. (2020) 144640. https://doi.org/10.1016/j.apsusc.2019.144640
19. X. He et al., Assessment of nitrogen–fluorine-codoped TiO_2 under visible light for degradation of BPA: Implication for field remediation, 314, (2016) 81-92. https://doi.org/10.1016/j.jphotochem.2015.08.014
20. S. Sambaza, A. Maity, and K. J. J. o. E. C. E. Pillay, Enhanced degradation of BPA in water by PANI supported Ag/TiO_2 nanocomposite under UV and visible light, 7, 1, (2019) 102880. https://doi.org/10.1016/j.jece.2019.102880
21. X. Hao, M. Li, L. Zhang, K. Wang, C. J. J. o. i. Liu, and e. chemistry, Photocatalyst TiO_2/WO_3/GO nano-composite with high efficient photocatalytic performance for BPA degradation under visible light and solar light illumination, 55, (2017) 140-148,. https://doi.org/10.1016/j.jiec.2017.06.038
22. C. Y. Kuo, Y. H. Yang, H. M. Hsiao, and S. C. Liao, Photodegradation of Bisphenol A (BPA) by carbon doped TiO_2 under sunlight irradiation, in Applied Mechanics and Materials, , 378, (2013) 121-124. https://doi.org/10.4028/www.scientific.net/AMM.378.121
23. A. M. Cardenas-Peña, J. G. Ibanez, and R. J. I. J. E. S. Vasquez-Medrano, Determination of the point of zero charge for electrocoagulation precipitates from an iron anode, 7, 7, (2012) 6142-6153. http://ri.ibero.mx/handle/ibero/2105
24. H.-H. Huang, D.-H. Tseng, and L.-C. J. J. o. H. M. Juang, Heterogeneous photocatalytic degradation of monochlorobenzene in water, 156, 1-3, (2008) 186-193. ttps://doi.org/10.1016/j.jhazmat.2007.12.013
25. C. Shifu, C. J. S. Gengyu, and C. Technology, The effect of different preparation conditions on the photocatalytic activity of TiO_2· SiO_2/beads, 200, 11, (2006) 3637-3643. https://doi.org/10.1016/j.surfcoat.2004.11.025
26. P. Klankaw, C. Chawengkijwanich, N. Grisdanurak, S. J. S. Chiarakorn, and Microstructures, The hybrid photocatalyst of TiO_2–SiO_2 thin film prepared from rice husk silica, 51, 3, (2012) 343-352. https://doi.org/10.1016/j.spmi.2011.12.004
27. I. Levchuk, M. Sillanpää, C. Guillard, D. Gregori, D. Chateau, and S. J. A. S. S. Parola, TiO_2/SiO_2 porous composite thin films: Role of TiO_2 areal loading and modification with gold nanospheres on the photocatalytic activity, 383, (2016) 367-374. https://doi.org/10.1016/j.apsusc.2016.04.008
28. L. Yanyan, T. A. Kurniawan, Z. Ying, A. B. Albadarin, and G. J. J. o. M. L. Walker, Enhanced photocatalytic degradation of acetaminophen from wastewater using $WO_3/TiO_2/SiO_2$ composite under UV–VIS irradiation, 243, (2017) 761-770,. https://doi.org/10.1016/j.molliq.2017.08.092
29. S. Yaparatne, C. P. Tripp, and A. J. J. o. h. m. Amirbahman, Photodegradation of taste and odor compounds in water in the presence of immobilized TiO_2-SiO_2 photocatalysts, 346, (2018) 208-217. https://doi.org/10.1016/j.jhazmat.2017.12.029
30. A. Aizat et al., Photocatalytic degradation of phenol by $LaFeO_3$ nanocrystalline synthesized by gel combustion method via citric acid route, 1, 1, (2019) 91. https://doi.org/10.1007/s42452-018-0104-x
31. N. Jallouli, K. Elghniji, H. Trabelsi, and M. J. A. j. o. C. Ksibi, Photocatalytic degradation of paracetamol on TiO_2 nanoparticles and TiO_2/cellulosic fiber under UV and sunlight irradiation, 10, (2017) S3640-S3645,. https://doi.org/10.1016/j.arabjc.2014.03.014
32. M. F. Atitar, R. Dillert, and D. W. J. T. J. o. P. C. C. Bahnemann, Surface interactions between Imazapyr and the TiO_2 surface: An in situ ATR-FTIR study, 121, 8, (2017) 4293-4303. https://doi.org/10.1021/acs.jpcc.6b11673
33. A. Abdelhaleem and W. J. J. o. h. m. Chu, Photodegradation of 4-chlorophenoxyacetic acid under visible LED activated N-doped TiO_2 and the mechanism of stepwise rate increment of the reused catalyst, 338, (2017) 491-501. https://doi.org/10.1016/j.jhazmat.2017.05.056
34. M. Blanco-Vega et al., Photocatalytic elimination of bisphenol A under visible light using Ni-doped TiO_2 synthesized by microwave assisted sol-gel method, 71, (2017) 275-282,. https://doi.org/10.1016/j.mssp.2017.08.013
35. M. Khatamian and Z. J. D. Alaji, Efficient adsorption-photodegradation of 4-nitrophenol in aqueous solution by using ZnO/HZSM-5 nanocomposites, 286, (2012) 248-253,. https://doi.org/10.1016/j.desal.2011.11.031